

## Prognostic image-based quantification of CD8CD103 T cell subsets in high-grade serous ovarian cancer patients

S. T. Paijens<sup>a\*</sup>, A. Vledder<sup>a\*</sup>, D. Loiero<sup>b\*</sup>, E. W. Duiker<sup>c</sup>, J. Bart<sup>c</sup>, A. M. Hendriks<sup>d</sup>, M. Jalving<sup>d</sup>, H. H. Workel<sup>a</sup>, H. Hollema<sup>c</sup>, N. Werner<sup>c</sup>, A. Plat<sup>a</sup>, G. B. A. Wisman<sup>d</sup>, R. Yigit<sup>a</sup>, H. Arts<sup>a</sup>, A. J. Kruse<sup>e</sup>, N.M. de Lange<sup>e</sup>, V. H. Koelzer<sup>b#</sup>, M. de Bruyn<sup>a#</sup>, and H. W. Nijman<sup>d</sup>

<sup>a</sup>Department of Obstetrics and Gynecology, University of Groningen, University Medical Center Groningen, Groningen, The Netherlands; <sup>b</sup>Department of Pathology and Molecular Pathology, University Hospital and University of Zurich, Zurich, Switzerland; <sup>c</sup>Department of Pathology, University of Groningen, University Medical Center Groningen, Groningen, The Netherlands; <sup>d</sup>Department of Medical Oncology, University of Groningen, University Medical Center Groningen, Groningen, The Netherlands; <sup>e</sup>Department of Obstetrics and Gynecology, Isala Hospital Zwolle, Zwolle, The Netherlands

### ABSTRACT

CD103-positive tissue resident memory-like CD8<sup>+</sup> T cells (CD8CD103 TRM) are associated with improved prognosis across malignancies, including high-grade serous ovarian cancer (HGSOC). However, whether quantification of CD8, CD103 or both is required to improve existing survival prediction and whether all HGSOC patients or only specific subgroups of patients benefit from infiltration, remains unclear. To address this question, we applied image-based quantification of CD8 and CD103 multiplex immunohistochemistry in the intratumoral and stromal compartments of 268 advanced-stage HGSOC patients from two independent clinical institutions. Infiltration of CD8CD103 immune cell subsets was independent of clinicopathological factors. Our results suggest CD8CD103 TRM quantification as a superior method for prognostication compared to single CD8 or CD103 quantification. A survival benefit of CD8CD103 TRM was observed only in patients treated with primary cytoreductive surgery. Moreover, survival benefit in this group was limited to patients with no macroscopic tumor lesions after surgery. This approach provides novel insights into prognostic stratification of HGSOC patients and may contribute to personalized treatment strategies in the future.

### ARTICLE HISTORY

Received 27 March 2021  
Revised 20 May 2021  
Accepted 20 May 2021

### KEYWORDS



CD8CD103 t cell; tissue resident memory t cells; high grade serous ovarian cancer; digital quantification; prognosis; overall survival

## Introduction

High-grade serous ovarian cancer (HGSOC) is the most common histological subtype of epithelial ovarian cancer (EOC) and considered to originate from the fallopian tubes.<sup>1</sup> Advanced stage HGSOC has a poor prognosis, with a 5-year survival rate of 25–40%.<sup>2,3</sup> Current primary treatment consists of cytoreductive surgery and chemotherapy, in most cases carboplatin with paclitaxel.<sup>4</sup> Patients are either treated with primary debulking surgery followed by six cycles of adjuvant chemotherapy (PDS) or are initially treated with three cycles of neo-adjuvant chemotherapy, followed by interval debulking surgery and three additional cycles of adjuvant chemotherapy (NACT). Choice of treatment strategy is tailored for each individual patient. Patients are selected for PDS based on the estimation whether the entire tumor load can be removed during surgery, taking into account tumor location, presence of metastases and clinical condition of the patient. If not feasible, NACT is used to reduce tumor burden prior to interval debulking. The most important prognostic factors are primary treatment strategy (PDS or NACT) and surgical outcome. Surgical outcome is defined as complete (no residual macroscopic tumor tissue after surgery), optimal (residual

tumor lesions <1 cm after surgery) or incomplete (residual tumor lesions >1 cm after surgery). Although up to 75% of all HGSOC patients initially have a favorable response to primary treatment, comprising chemotherapy and surgery, most patients relapse within 2 years, with a median progression-free survival (PFS) of 12 months.<sup>5</sup>

It has been well established that the presence of tumor infiltrating lymphocytes (TILs) represents an additional favorable prognostic indicator in many solid tumors including HGSOC.<sup>6–8</sup> In particular, a specific subset of CD8<sup>+</sup> T cells, known as tissue resident memory-like T cells (TRM), is associated with prognostic benefit in HGSOC.<sup>9–11</sup> TRM are characterized by the expression of CD103, also known as integrin  $\alpha E\beta 7$  (*ITGAE*). CD103 interacts with E-cadherin, often expressed on epithelial tumor cells, thereby facilitating the interaction between the CD8<sup>+</sup> T cells and the tumor epithelium. CD103 is therefore often used to distinguish intra-epithelial and stromal CD8<sup>+</sup> T cells.<sup>12</sup> Functional studies have shown that CD8CD103 TRM cells can secrete pro-inflammatory cytokines such as Interferon- $\gamma$  (IFN $\gamma$ ), tumor necrosis factor- $\alpha$ , and express cytotoxic molecules granzyme A and B.<sup>13,14</sup> In addition, as previously demonstrated by our group, CD8CD103 TRM cells also produce CXCL13, a crucial

**CONTACT** H. W. Nijman  [h.w.nijman@umcg.nl](mailto:h.w.nijman@umcg.nl)  Department of Obstetrics and Gynecology, University of Groningen, University Medical Center Groningen, CMC V, 4e floor room Y4.242, PO 30.001, Groningen 9700 RB, The Netherlands

\*These authors contributed equally to this work

#Shared senior authorship

 Supplemental data for this article can be accessed on the [publisher's website](#)

© 2021 The Author(s). Published with license by Taylor & Francis Group, LLC.

This is an Open Access article distributed under the terms of the Creative Commons Attribution-NonCommercial License (<http://creativecommons.org/licenses/by-nc/4.0/>), which permits unrestricted non-commercial use, distribution, and reproduction in any medium, provided the original work is properly cited.

chemokine involved in the development of tertiary lymphoid structures (TLS).<sup>15</sup>

In order to translate CD8CD103 TRM quantity and location into a diagnostic tool, the development of immune scores are needed. However, manual TIL quantification by pathologists is hampered by interobserver variability and is time-consuming.<sup>16</sup> The rise of digital pathology, including image-based quantification and machine learning algorithms, provides an opportunity to overcome these limitations. Machine learning algorithms apply statistical methods to process data and have shown to be reproducible and reliable for the analysis of tissue composition in cancer.<sup>17</sup> The deep characterization of the tumor microenvironment, through spatial analysis and multiplexing, makes image-based quantification an efficient tool to extract comprehensive information on biomarker expression levels, colocalization, and compartmentalization.<sup>18,19</sup> Horeweg et al. demonstrated the successful application of image-based CD8CD103 TRM quantification in early-stage endometrial cancer, by demonstrating concordance between automatic machine learning and assessment by expert pathologists. The study showed greater sensitivity of automatic machine learning compared to manual quantification.<sup>20</sup>

In this study, we applied the same innovative image-based quantification technique as Horeweg et al. to address the questions; whether CD8, CD103 or both markers need to be quantified for optimal prognostication in HGSOE; and whether all HGSOE patients or only specific subgroups of patients benefit from infiltration. We demonstrate that the prognostic benefit of CD8CD103 TRM infiltration in HGSOE is restricted to PDS treated patients with a complete debulking.

## Methods

### Patient selection

A recoded database was created containing information on clinico-pathological characteristics and follow-up of patients diagnosed with advanced stage HGSOE at the University Medical Center Groningen (Groningen, The Netherlands) and Isala hospital Zwolle (Zwolle, The Netherlands) between January 2008 and January 2017. Patients were staged according to international Federation of Gynecology and Obstetrics (FIGO) criteria 2014 based on World Health Organization (WHO) guidelines.

One of the gynecologic pathologist (EWD, JB, NW, HH) confirmed the histological subtype based on morphology, and when available P53 immunohistochemistry staining. Subsequently, the presence of tumor tissue was confirmed on H&E slides and representative locations with tumor tissue were selected for tissue microarray (TMA) construction. Patients were included if sufficient formalin-fixed paraffin embedded (FFPE) ovarian or omentum tumor tissue was available. Tissue was obtained either from primary debulking surgery or interval debulking surgery.

From a total of 409 patients that were screened, 268 patients (65.5%) were included, follow-up survival data were available for 240 included patients of which 2 patients had an unknown surgical outcome. Of the 141 excluded patients follow-up, survival data were available for 92 of the patients

(Supplementary Figure 1). The main reason for exclusion was the unavailability of viable tumor tissue. Approximately 80% of the excluded patients were primarily treated with NACT (Supplementary Table 1). Since these excluded NACT patients might represent 'best responders to chemotherapy', we analyzed overall survival (OS) in the exclusion versus inclusion cohort. We observed a prolonged survival for the included NACT patients compared to the excluded NACT patients (Supplementary Figure 2(b)). Within PDS-treated patients, no difference in OS was observed between included or excluded patients (Supplementary Figure 2(a)).

In total (n = 268), FFPE tissue of 191 advanced-stage HGSOE patients at the UMCG and 77 HGSOE patients at the Isala was available for the construction of a TMA. For 210 patients both infiltration density and survival data were available, of which 2 patients had an unknown surgical outcome (Supplementary Figure 1). OS was calculated from the date of initial treatment (either primary surgery or first cycle of neo-adjuvant chemotherapy) and was last updated in July 2020.

### Tissue micro-array

Triplicate cores with a diameter of 1 mm were taken from each FFPE block and placed in a recipient block using a tissue microarrayer (Beecher instruments, Silver Spring, USA). Both normal and tumor tissue were included as orientation cores and controls. From each TMA block, 3- $\mu$ m-thick sections were cut and applied to APES-coated slides (Starfrost, Braunschweig, Germany).

### Immunohistochemistry staining

FFPE slides were de-paraffinized and rehydrated in graded ethanol. Antigen retrieval was initiated with a preheated 10 mM citrate buffer (pH = 6). Endogenous peroxidase was blocked with a 0.3% H<sub>2</sub>O<sub>2</sub> solution (0.5 mL 30% H<sub>2</sub>O<sub>2</sub> in 50 mL PBS) for 30 minutes at room temperature. The primary antibodies against CD8 (1:50, Agilent/Dako, M710301-2) and CD103 (1:200, CD103; ab129202) were diluted in phosphate buffered saline (PBS)(PBS + 1% BSA + 1% AB serum; total 80  $\mu$ L) and, slides were incubated overnight at 4°C. Next, the slides were incubated with two secondary antibodies, first with envision +/HRP anti-rabbit (2 drops, K400311-2P), followed by secondary antibody immPRESS-AP mouse (MP-5402-15), both for 30 min at room temperature. For visualization, StayYellow/HRP (Abcam, ab169561) and Fast Red Substrate kit (Abcam, ab64254) were used according to manufacturers' instructions. Appropriate washing steps with PBS, tris-buffered saline with 0,1% Tween and demi water were performed between incubation steps. Sections were mounted with Eukitt quick-hardening mounting medium (Sigma Aldrich, Steinheim, Germany), and scanned on a Hamamatsu digital slide scanner (Hamamatsu photonics, Hamamatsu, Japan). Representative staining images are depicted in supplementary Figure 3.

### Image-based quantification of CD8CD103 immune cell subsets

All digital slides were reviewed by two pathologists (DL and VHK) and spots with staining artifacts, folds or less than 50%

viable tissue/core were excluded from analysis. The digital image analysis was carried out using HALO digital image analysis software version v3.0.311.167 (Indica Labs, Corrales, NM, USA). Specifically, TMA slides were de-arrayed into individual spot images of each tissue sample linked to clinical annotations. To localize and quantify tumor and stroma tissue, a deep neural network algorithm was trained using the Deep Net architecture. Necrosis, erythrocyte aggregates, and glass background were excluded. Graphical overlays were generated for each tissue class and the classification accuracy was reviewed. The total area of each tissue class was quantified in  $\text{mm}^2$ . Cell detection, segmentation and staining quantification for Nuclei (Hematoxylin, RGB 57, 49, 137), CD8 (Fast Red, RGB 203, 64, 122), and CD103 (StayYellow, RGB 216, 173, 81) were performed in the tumor and stromal compartment. CD8 and CD103 were classified as positive if staining intensity in the cytoplasmic compartment exceeded internal controls (nonimmune cells in same tissue) as validated by pathologist review. The total tissue area in the tumor and stromal compartment and the absolute and % number of CD8 and CD103 single and double-positive cells were recorded (Figure 1). CD8 and CD103 infiltration density (marker-positive cells/ $\text{mm}^2$ ) was calculated across all cores of each individual case and analyzed with clinico-pathological parameters.

### Statistical analysis

Statistical analyses were performed using IBM SPSS Statistics for Windows, version 23 (IBM Corp., Armonk, N.Y., USA) and R (version 3.6.2). For analysis, immune cell densities were log2 transformed. Clustering of cases was done by hierarchical clustering using Ward's minimum variance method in R using package pheatmap (<https://cran.r-project.org/web/packages/pheatmap/index.html>). Correlations between CD8CD103 TRM cells and clinical and histopathological variables were analyzed using Multiple regression analysis in SPSS. Independent prognostic value of CD8CD103 TRM cells was analyzed using Multivariate Cox analysis in SPSS. Analyses of OS as a function of immune cell density were performed by Cox proportional hazards models in R using packages RMS (<https://cran.r-project.org/web/packages/rms/index.html>) and survival (<https://cran.r-project.org/web/packages/survival/index.html>), and plotted using package ggPlot2 (<https://cran.r-project.org/web/packages/ggplot2/index.html>). Proportionality of hazards was confirmed by scaled Schoenfeld residuals. Exploratory analysis of the optimal cutoff was determined in R using package Survminer <https://cran.r-project.org/web/packages/survminer/index.html>. Survival curves were plotted in R using Survminer by using the Kaplan–Meier method. A *p*-value of <0.05 was used as cutoff for significance.

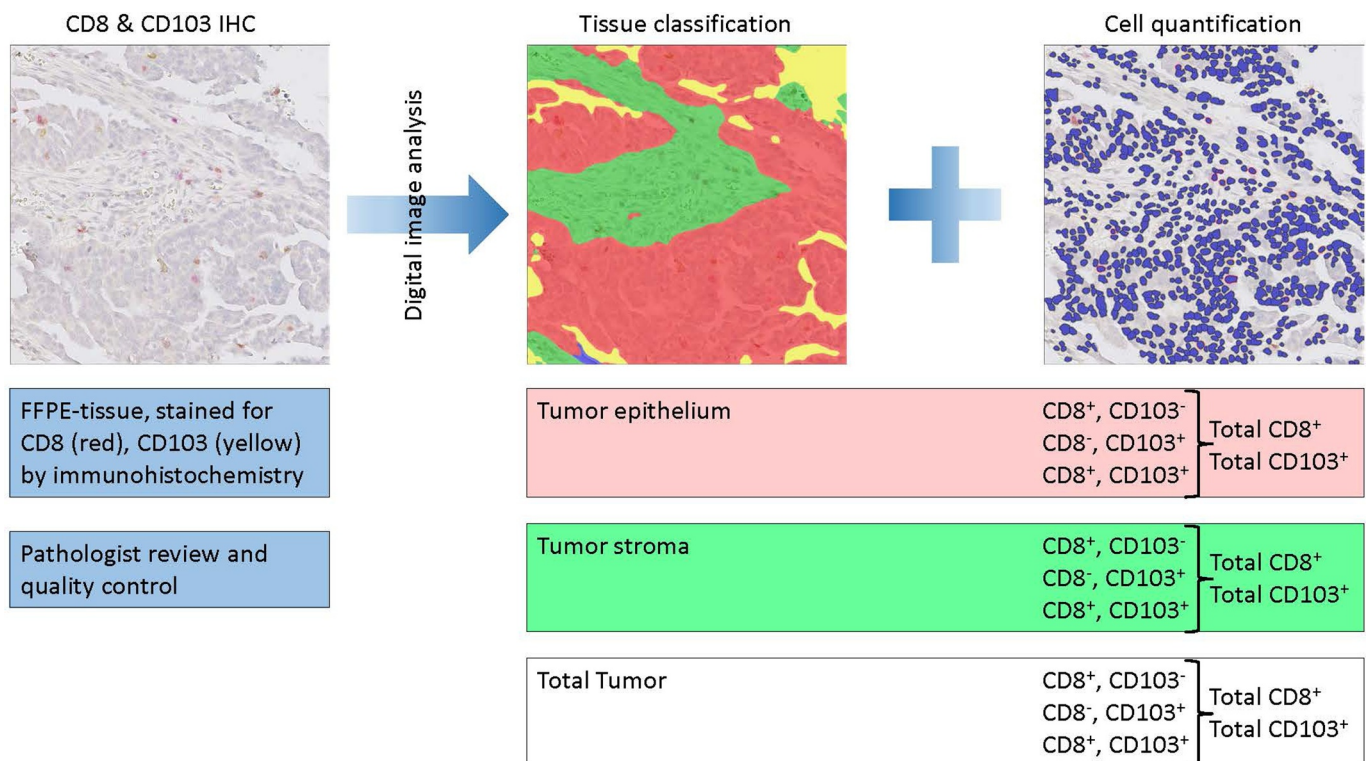


**Figure 1. Schematic illustration of CD8CD103 quantification method.** A digital image of CD8CD103 multiplex immunohistochemistry stained tissue was analyzed using a deep neural network algorithm, trained to distinguish the epithelial and stromal compartments. Stromal and epithelial compartments were combined to assess the unsegmented tissue (intratumoral). Quantification of CD8<sup>+</sup>CD103<sup>-</sup> (single CD8) and CD8<sup>-</sup>CD103<sup>+</sup> (single CD103) and double positive CD8<sup>+</sup>CD103<sup>+</sup> (CD8CD103 TRM) cells were recorded. Single CD8 and CD103 infiltration density (marker-positive cells /  $\text{mm}^2$ ) was calculated across all cores of each individual case. All scores were integrated into 15 endscores.

## Ethical review

Patient data were retrieved from the institutional database into a new recoded database, in which patient identity was protected by unique patient codes. According to Dutch law, the institutional review board approved the use of the no-objection procedure for further-use biobank and databank (METc 2018.543).

## Results

### Cohort description

In total, 268 advanced-stage HGSOc patients were included. Patient characteristics from the two participating centers were compared and no significant difference was observed for FIGO stage, primary treatment and chemotherapy regimen (Table 1). OS did not differ between the two cohorts ( $p = .15$ ; *data not shown*). BRCA-testing for EOC has only become standard of care since 2019 and is therefore largely unknown in our cohort and not compared for both centers. Based on the similar characteristics, both hospital cohorts were subsequently analyzed as one group.

Since patients are selected for primary treatment strategy (PDS or NACT) based on tumor burden, tumor location and health status, and therefore not comparable, the effect on OS was assessed independently for both patient groups. Additionally, we corrected for surgical outcome, since this is

the main prognostic factor in HGSOc patients. Indeed, survival analysis revealed a significant benefit of the extent of cytoreductive surgery in PDS patients with survival outcomes of 58, 40 and 29 months in patients with a complete debulking versus an optimal or incomplete debulking, respectively ( $p < .01$ ). Additionally, optimally debulked PDS patients had a significantly better survival than incompletely debulked patients ( $p < .01$ ). In NACT patients, patients with a complete debulking had a significantly better survival outcome as compared to patients with an optimal or incomplete debulking of 39, 29 and 27 months, respectively ( $p < .01$ ) (Supplementary Figure 4, Supplementary Table 3).

### Patterns of infiltration of the CD8CD103 immune cell subsets

Infiltration of three immune cell subsets was assessed; CD8<sup>+</sup>CD103<sup>-</sup> (single CD8), CD8<sup>-</sup>CD103<sup>+</sup> (single CD103) and CD8<sup>+</sup>CD103<sup>+</sup> TRM cells (CD8CD103 TRM) in different locations; the epithelium and stromal compartments (Figure 1).<sup>20</sup> Hierarchical clustering revealed that patients were clustered together based on infiltration of the various cell subsets, independent of location (Figure 2(a)). In addition, there was apparent heterogeneity in the degree of single CD8, single CD103 and CD8CD103 TRM infiltration with a subgroup of patient samples infiltrated by single CD8 cells or single CD103 cells, but not CD8CD103 TRM cells. By contrast, most patient samples with a high level of CD8CD103 TRM infiltration were also characterized by a strong infiltrate of CD8 and CD103 single positive cells (Figure 2(a)). Multiple regression analysis revealed no significant association of FIGO stage, treatment strategy, or surgery outcome with any of the clusters or cell subsets (Figure 2(a)). Finally, multiple regression analysis of histopathological markers determined during diagnostic workup (p53, p16, PAX8, WT1 and CK7) revealed no particular association with the CD8CD103 TRM immune clusters (Figure 2(b)).

### Prognostic benefit of stromal and epithelial CD8CD103 TRM infiltration

To determine which immune cell subset contributed to increased survival of the complete HGSOc patient population, we analyzed hazard ratios for all cell subsets in both the epithelial and stromal compartment (Figure 3(a)). Only CD8CD103 TRM in the epithelium were associated with improved survival (HR: 0.87,  $p = .056$  and Figure 3(a,b)). Accordingly, exploratory analysis of survival at an optimal cutoff (top 15%) revealed a clear survival benefit for patients with high tumor epithelial CD8CD103 TRM infiltration (Figure 3(c)). In line with previous publications,<sup>21</sup> we also assessed the survival benefit using the highest tertile for cutoff (Supplementary Table 4), which revealed a survival benefit for patients with tumor epithelial high CD8CD103 TRM infiltration ( $p = .01$ , Figure 3(d)).

Next, we explored survival in PDS and NACT patients as independent groups, since these two primary treatment strategies are not directly comparable. We corrected for surgical outcome through comparison of patients with no macroscopic lesions after surgery (complete debulking) and patients with

**Table 1.** Patient characteristics inclusion cohort.

		UMCG (N = 191)		Isala (N = 77)		P-value
		N	%	N	%	
Mean age at diagnosis		65		63		
FIGO stage <sup>a</sup>	IIB/IIC	9	4.7	4	5.2	.89
	III	142	74.3	58	75.3	
	IV	40	20.9	14	18.2	
	Unknown	0	0.0	1	1.3	
BRCA status	BCRA1/ BRCA2 mutation	12	6.3	12	15.6	N/A
	No BCRA mutation	74	38.7	12	15.6	
	Unknown	105	55	53	68.8	
Primary treatment	PDS	61	68.5	20	58.8	.53
	Optimal	12	13.5	5	14.7	
	Incomplete	16	18.0	7	2.4	
	Unknown	0	0	2	5.9	
	NACT	34	33.3	23	54.8	.01
	Optimal	39	38.2	9	21.4	
	Incomplete	29	28.4	9	21.4	
	Unkown	0	0	1	2.4	
NACT regime	Carboplatin/Paclitaxel	97	95.1	40	95.2	.97
	Other/Unknown	5	4.9	2	4.8	
AC regime	Carboplatin/Paclitaxel	153	80.1	67	87.0	.35
	No chemotherapy	13	6.8	2	2.6	
	Other/Unknown	25	13.1	8	10.4	
Disease status <sup>a</sup>	Evidence of disease	142	74.3	49	63.6	.01
	No evidence of disease	27	14.1	15	19.5	
	Progressive disease during primary treatment	7	3.7	11	14.3	
	Unknown	15	7.9	2	2.6	

**FIGO:** Fédération Internationale de Gynécologie et d'Obstétrique.

**PDS:** Primary debulking surgery followed by 6 cycles of adjuvant chemotherapy;

**NACT:** 3 cycles of neo-adjuvant chemotherapy, followed by an interval debulking and 3 cycles adjuvant chemotherapy.

**Complete:** all visible tumor lesions were removed; **Optimal:** tumor lesion left <1 cm; **Incomplete:** tumor lesions left >1 cm.

<sup>a</sup>Chi-square  $p$ -value excluded "Unknown/missing".

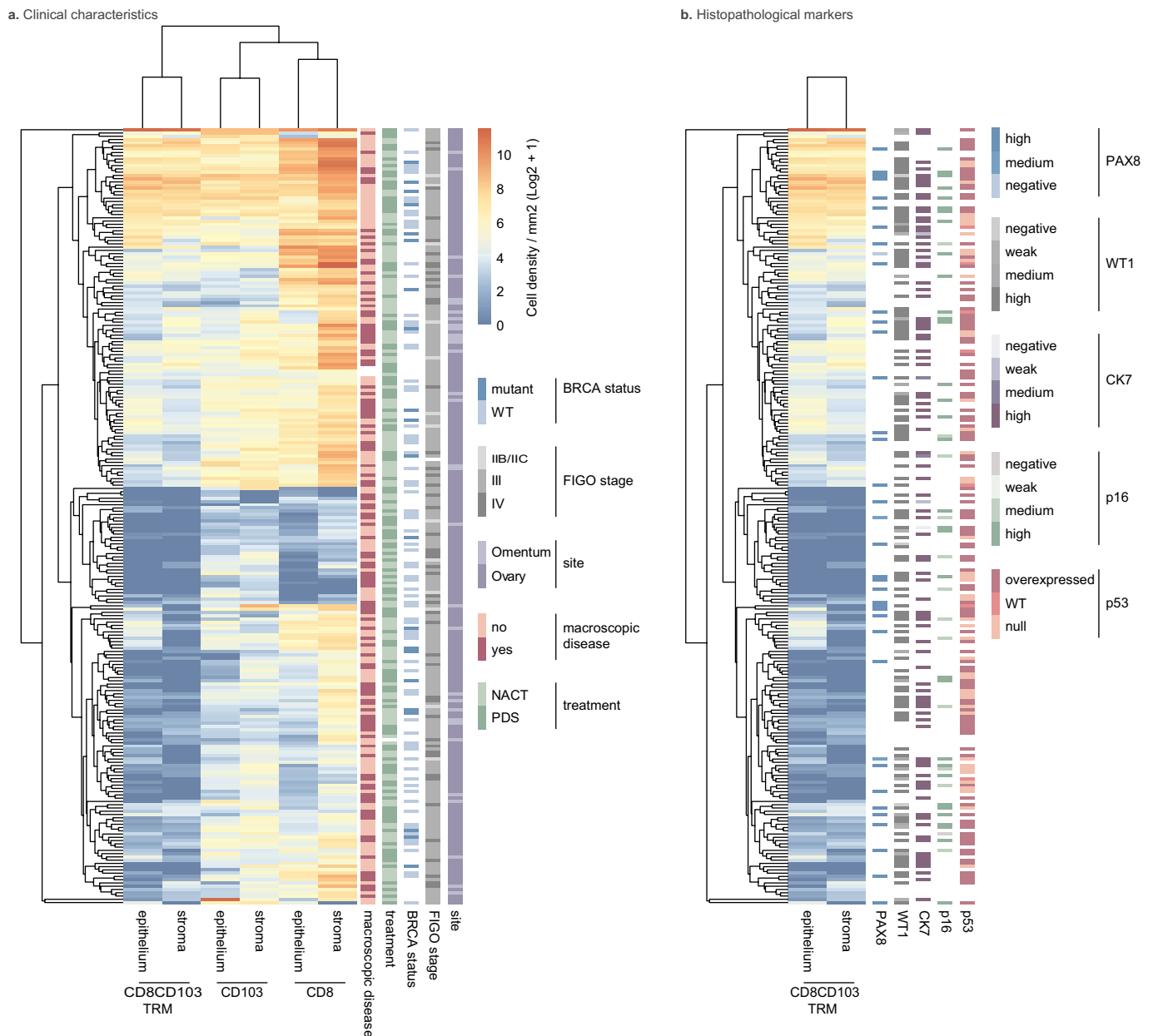


**Figure 2. Patterns of infiltration of the CD8CD103 immune cell subsets.** **A**, Heatmap displaying infiltration of the CD8CD103 immune cell subsets in the epithelium and stromal compartment. Hierarchical cluster analysis of all samples displayed three main clusters based on immune cell population; CD8<sup>+</sup>CD103<sup>+</sup> (CD8CD103 TRM); CD8<sup>+</sup>CD103<sup>-</sup> (single CD103) and CD8<sup>+</sup>CD103<sup>-</sup> (single CD8). For each sample clinical characteristics are displayed including BRCA-status, FIGO-stage, site of tumor material collection, presence of macroscopic disease after surgery and primary treatment strategy. **B**, Heatmap of the CD8CD103 TRM immune cell cluster determined in figure 1A, displaying the analysis of histopathological markers determined during diagnostic workup including p53, PAX8, WT1 and CK7.

macroscopic tumor lesions after surgery (optimal/incomplete debulking). To allow for sufficient numbers of patients in the subanalysis, we chose the highest tertile as cutoff. In the PDS cohort, patients with no macroscopic tumor lesions after surgery and high CD8CD103 TRM infiltration in the tumor epithelium or stroma were characterized by a significantly longer survival than patients with no macroscopic tumor lesions and low CD8CD103 TRM infiltrate (Figure 4(a), 5-year survival 83% versus 52%;  $p = .03$  and Figure 4(b), 5-year survival 77% versus 54%;  $p = .01$ , respectively). In the NACT cohort, there was no effect of CD8CD103 TRM infiltration on OS in patients with and without macroscopic tumor

lesions after surgery in stroma or tumor epithelium (Figure 4(c),  $p = .77$  and Figure 4(d),  $p = .32$ ).

### Prognostic benefit of CD8CD103 TRM cell infiltration in unsegmented tissue

The pipeline used in the current study leverages both tissue segmentation and cell identification using machine learning algorithms. We next evaluated whether analysis of unsegmented tissue would provide comparable prognostic benefit and potentially accelerate future clinical workflows. Hereto, we analyzed survival of patients stratified by single CD8, single CD103 or

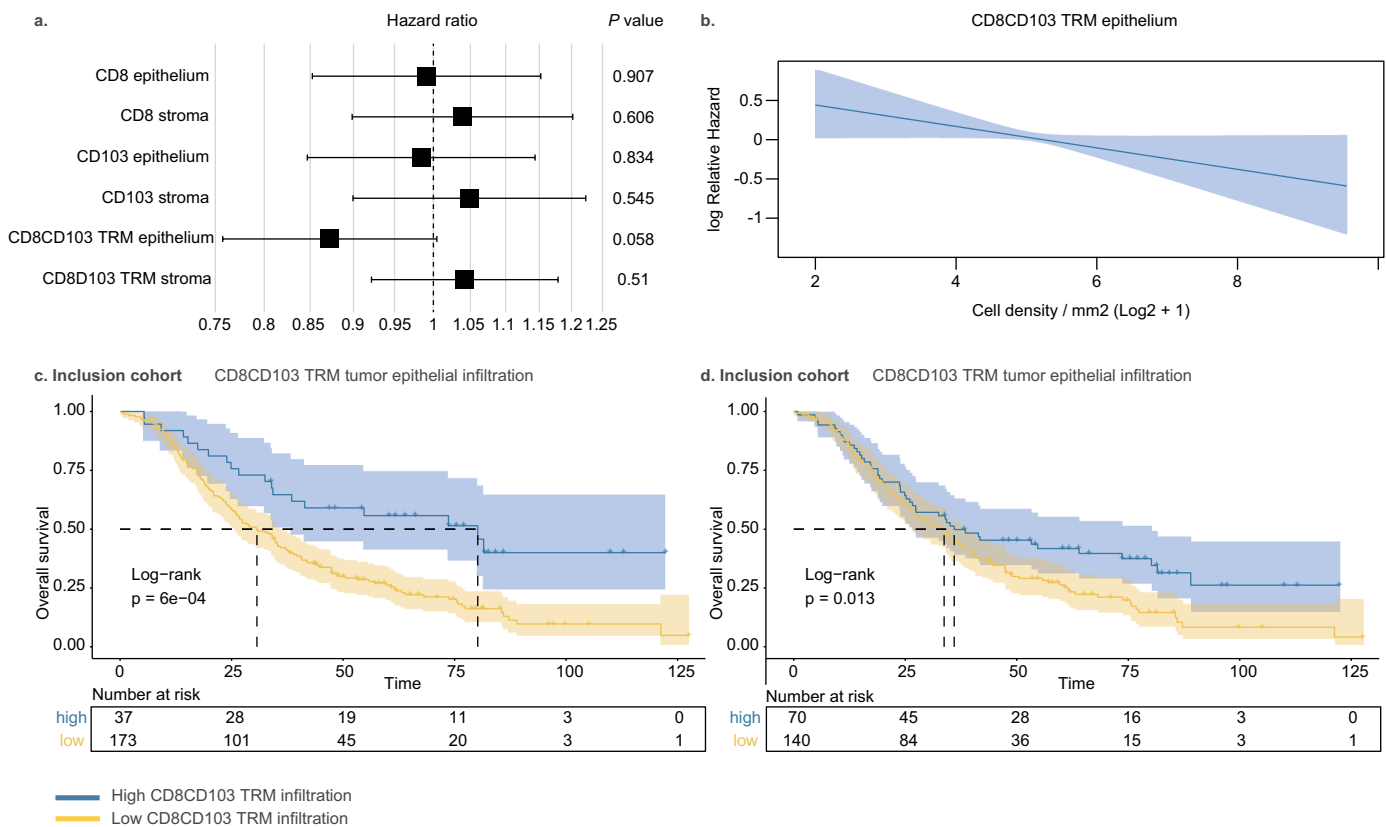


**Figure 3. Prognostic benefit of stromal and epithelial CD8CD103 TRM infiltration in all patients.** **A**, Forest plot of hazard ratios displaying stromal and epithelial infiltration of the three main CD8CD103 immune cell subsets; single CD8, single CD103 and CD8CD103 TRM. Only, epithelial CD8CD103 TRM infiltration is associated with improved survival. **B**, Plot showing hazard ratio for overall survival (OS) according to log<sub>2</sub> transformed density of intra-epithelial CD8CD103 TRM cells. **C**, OS was determined in patients with high versus low epithelial CD8CD103 TRM infiltration based on the optimal cut-off ( $p < 0.01$ ). Survival differences were determined by a log-rank test. Numbers at risk are specified in the figure. **D**, OS was determined in patients with high versus low epithelial CD8CD103 TRM infiltration based on the highest tertile ( $p = 0.01$ ). Survival differences were determined by a log-rank test. Numbers at risk are specified in the figure.

CD8CD103 TRM in the total patient cohort. Only CD8CD103 TRM was associated with survival benefit when analyzing unsegmented tissue ( $p = .01$ ) (Figure 5(a)). In addition, neither total CD8 (HR 1.02 [0.92–1.1],  $p = .76$ ) nor total CD103 (HR 0.92 [0.80–1.1],  $p = .23$ ) were associated with improved survival. Analysis by log-rank test using either the optimal cutoff or the top tertile confirmed prognostic benefit for highly infiltrated patients (Figure 5(c,d), respectively). Exploratory sub-analysis of CD8CD103 TRM in the individual patient groups again revealed the restriction of prognostic benefit to PDS patients with no macroscopic tumor tissue (Figure 5(e)).

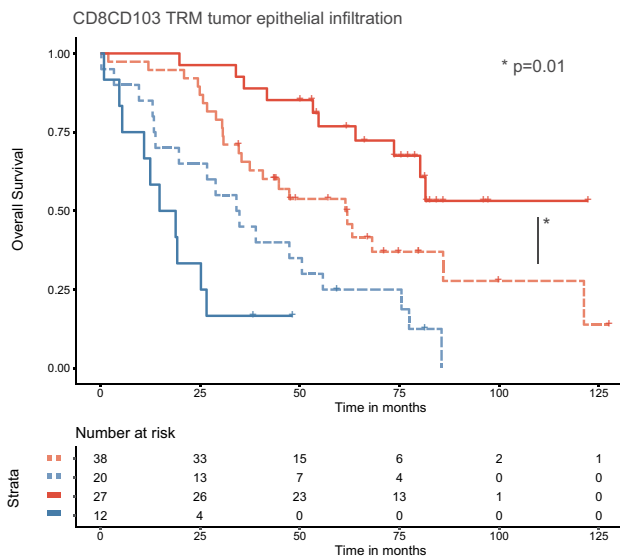
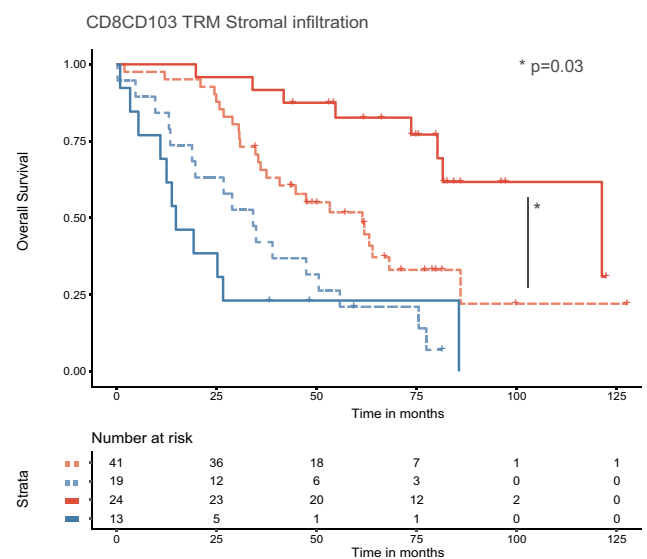
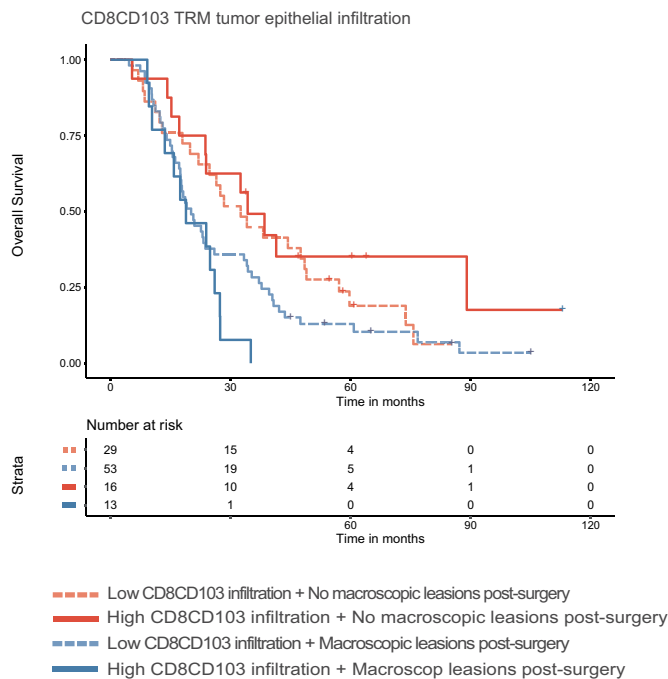
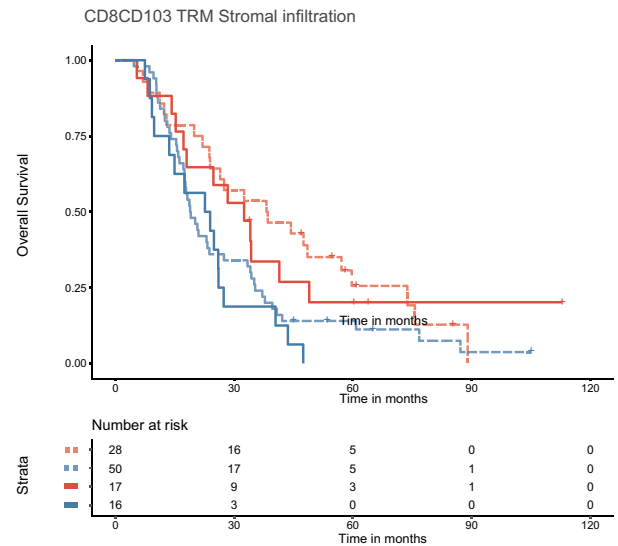
## Discussion

This study applies a digital quantification method,<sup>20</sup> employing deep neural networks for tissue segmentation, to determine the infiltration patterns of single CD8, single CD103 and CD8CD103 TRM in HGSOE, and to investigate the impact of the spatial distribution of immune cells in the tumor micro-environment on clinical outcomes. We demonstrate that high CD8CD103 TRM infiltration is associated with improved survival in HGSOE patients; however, this survival benefit is restricted to completely debulked PDS patients.

In line with previously published work, PDS patients with a complete debulking had the longest OS ( $\pm 58$  months),

followed by optimally debulked PDS patients and completely debulked NACT patients (both  $\pm 40$  months).<sup>21,22</sup> Importantly, the ~50% 5-year OS in PDS patients treated between 2008 and 2017 in this study was also comparable to other published data demonstrating a 44–56% 5-year OS in PDS patients treated between 2006 and 2013.<sup>22</sup> In our NACT cohort, time to recurrence and OS were approximately 13 and 31.8 months, which is a slightly inferior outcome than published by Cobb et al., who demonstrated a PFS of 16.4 and an OS of 48.2 months. However, in the recent analysis by Cobb et al., HGSOE patients were not randomly selected as they were matched to the investigated low-grade serous ovarian cancer patients. Hence, approximately two-third of the NACT patients had no tumor lesions post-surgery,<sup>23</sup> whereas in our study only one-third of the NACT patients had a complete interval debulking surgery.

In general, EOC is characterized by a relatively low mutational burden and low numbers of TILs compared to, for example, melanoma and lung cancer.<sup>24,25</sup> The present cohort confirms the overall low number of TILs in HGSOE with only 15% of the patients having high CD8CD103 TRM infiltrate, based on the optimal cutoff. Our results on the restricted prognostic benefit of CD8CD103 TRM to completely debulked PDS patients are in line with Zhang et al., who also reported

**a. Overall Survival PDS cohort****b. Overall Survival PDS cohort****c. Overall Survival NACT cohort****d. Overall Survival NACT cohort**

**Figure 4. Prognostic benefit of stromal and epithelial CD8CD103 TRM infiltration in patient subgroups.** (A-D), Overall survival (OS) differences were determined by Kaplan Meier analysis. Patients were stratified to high or low CD8CD103 TRM infiltration in the epithelial and stromal compartment using the highest tertile cut-off. Number at risk is specified in the figure. **A**, High versus low epithelial CD8CD103 TRM infiltration PDS patients with no macroscopic lesions after surgery ( $p=0.01$ ) and with macroscopic lesions after surgery ( $p=0.06$ ) **B**, High versus low stromal CD8CD103 TRM infiltration PDS patients with no macroscopic lesions after surgery ( $p=0.03$ ) and with macroscopic lesions after surgery ( $P=0.428$ ) **C**, High versus low epithelial CD8CD103 TRM infiltration NACT patients with no macroscopic lesions after surgery ( $p=0.32$ ) and with macroscopic lesions after surgery ( $p=0.13$ ) **D**, High versus low stromal CD8CD103 TRM infiltration NACT patients with no macroscopic lesions after surgery ( $p=0.77$ ) and with macroscopic lesions after surgery ( $p=0.42$ ).

prognostic benefit of TILs related to surgical outcome in ovarian cancer.<sup>26</sup> Why only this small subgroup of patients benefits from high CD8CD103 TRM infiltration remains unclear. Hypothetically, in patients with macroscopic tumor lesions after surgery, the remaining tumor load could exploit immune escape mechanisms, thereby suppressing CD8CD103 TRM activity. In NACT patients, no clear survival benefit was observed for patients with high TRM infiltration in either the

stromal or epithelial compartment, which is concordant with our previous work.<sup>21</sup> The absence of prognostic benefit of TILs in NACT patients has been observed in our previous research and could be explained by reduced MHC-I expression resulting in lack of CD8 T cell activation and reduced immunogenicity.<sup>27</sup> Indeed, chemotherapy has been associated with MHC-I down regulation in cancer.<sup>28</sup>

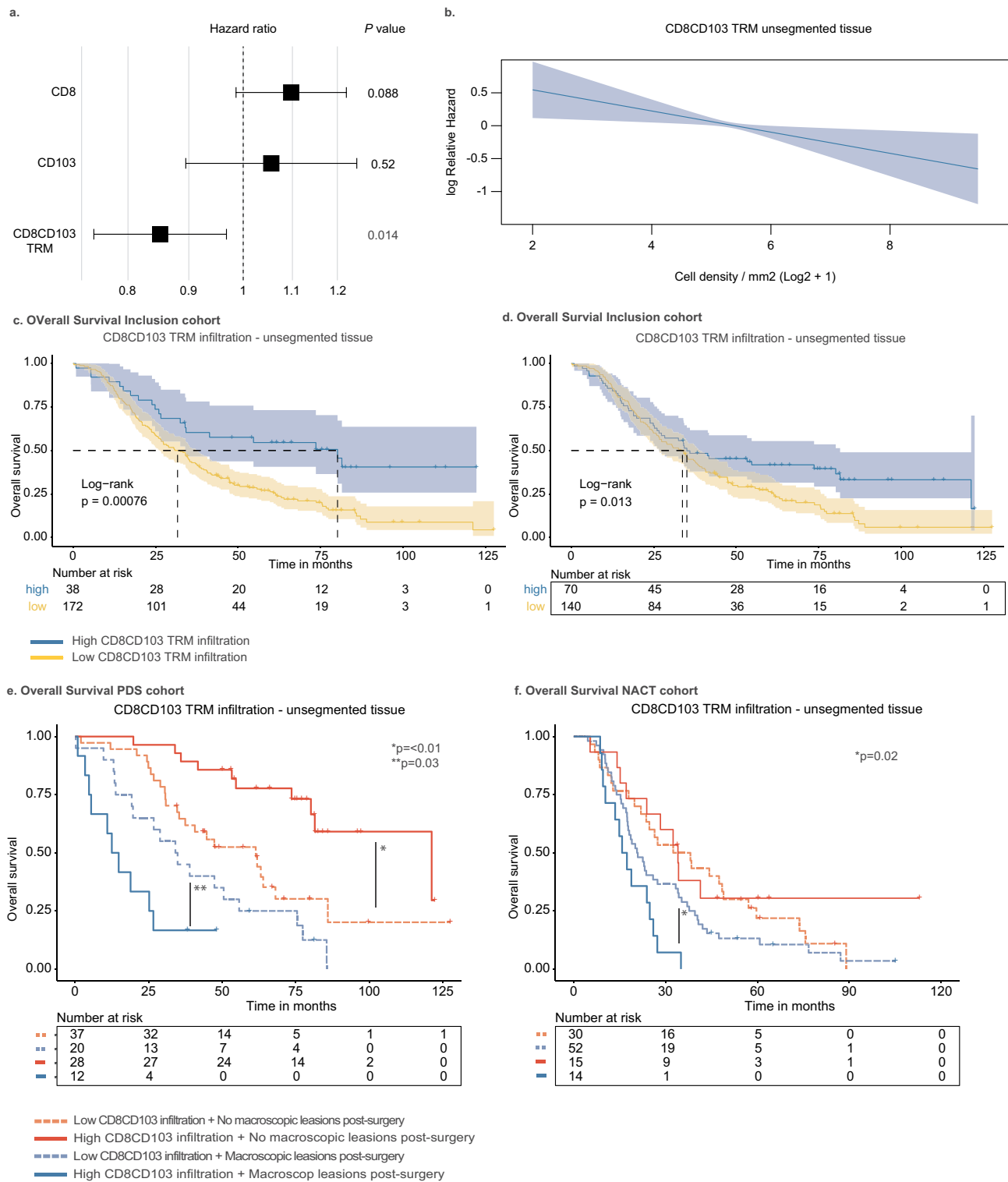


**Figure 5. Prognostic benefit of CD8CD103 TRM cell infiltration in unsegmented tissue.**(A-F), Displays analysis of infiltration in unsegmented tissue of the CD8CD103 immune cell subsets. **A**, Forest plot of hazard ratios displaying infiltration of the three main CD8CD103 immune cell subsets; single CD8, single CD103 and CD8CD103 TRM. Only, CD8CD103 TRM infiltration is associated with improved survival ( $p=0.014$ ). **B**, Plot showing hazard ratio for overall survival (OS) according to log2 transformed density of CD8CD103 TRM cells. **C**, OS was determined in patients with high versus low CD8CD103 TRM infiltration based on the optimal cut-off ( $p<0.01$ ). Survival differences were determined by a log-rank test. Numbers at risk are specified in the figure. **D**, OS was determined in patients with high versus low CD8CD103 TRM infiltration in unsegmented tissue based on the highest tertile ( $p=0.01$ ). Numbers at risk are specified in the figure. **(E-F)**, Survival differences were determined by Kaplan Meier analysis. Patients were stratified to high or low CD8CD103 TRM infiltration in unsegmented tissue using the highest tertile cut-off. Number at risk is specified in the figure. **E**, High versus low CD8CD103 TRM infiltration PDS patients with no macroscopic lesions after surgery ( $p<0.01$ ) and with macroscopic lesions after surgery ( $p=0.03$ ). **F**, High versus low CD8CD103 TRM infiltration NACT patients with no macroscopic lesions after surgery ( $p=0.59$ ) and with macroscopic lesions after surgery ( $p=0.02$ ).



As expected, CD8CD103 TRM quantification in the tumor epithelium had the strongest predictive value. However, not only epithelial but also stromal CD8CD103 TRM infiltration was predictive for improved survival. Since analysis of TMA slides provide a two-dimensional assessment of tissue architecture, it cannot be excluded that the stromal CD8CD103 TRM were not still located in close proximity to the tumor epithelium just below or above the cross-section of the assessed TMA-slide. Furthermore, a fraction of the stromal CD8CD103 TRM could also represent 'bystander' tissue resident memory T cells (*bystander-TRM*). *Bystander-TRM* are tumor-unspecific T cells, residing in lymphoid and non-lymphoid tissues and can contribute to the anti-tumor immune response via the delivery of common adjuvant viral peptides, resulting in the recruitment and accumulation of immune cells such as CD8<sup>+</sup> T cells and NK cells.<sup>29</sup>

In unsegmented tissue, CD8CD103 TRM were only associated with improved survival in PDS patients with no macroscopic tumor tissue remaining after debulking surgery and seemed equally prognostic compared to assessment of the tumor epithelium compartment alone. Consequently, assessment of CD8CD103 TRM in unsegmented tissue, and not in individual compartments, could potentially accelerate future clinical workflows, increasing clinical applicability. Of note, an inverse correlation was observed in unsegmented tissue of both PDS and NACT patients with macroscopic lesions after surgery; low infiltration had a better survival compared to high infiltration. In the PDS cohort, the group with low infiltration consisted out of 12 optimal and 8 incomplete surgeries compared to three optimal and nine incomplete in the highly infiltrated group, providing an explanation for this unexpected survival difference. In the NACT cohort, only 15 patients were characterized with high infiltration versus 53 patients with low infiltration. Unfortunately, group sizes were too small to independently analyze survival for all surgical outcomes.

The results found in this study could potentially be used to improve immune checkpoint inhibition (ICI) treatment response rates and pave the way for personalized treatment. Up to now, ICI has shown limited response rates of only 10–15% in OC.<sup>30</sup> However, these phase II clinical trials were performed in unstratified relapsed or platinum-resistant OC patients.<sup>31,32</sup> Recent studies in the primary setting suggest ICI treatment early-on might be superior compared to ICI after disease recurrence.<sup>33,34</sup> Thus, we would argue for the exploration of ICI maintenance therapy in HGSO patients, in combination with standard adjuvant chemotherapy. Patients could be further stratified based on TIL infiltration, as it is well-established that ICI is most effective in tumors infiltrated by a high number of TILs.<sup>35–37</sup> Completely debulked PDS patients with high CD8CD103 TRM infiltrated tumors might therefore particularly benefit from ICI maintenance treatment. Whereas patients with complete PDS and low CD8CD103 TRM infiltrated tumors, might benefit more from a combinatorial treatment regimen of anti-tumor vaccination and subsequent ICI. This was recently successfully demonstrated in melanoma patients receiving an antigen-encoding mRNA vaccine, targeting non-mutated tumor-associated antigens, alone or in combination with ICI. Interestingly, response rates were not

correlated with tumor associated antigen expression nor mutational burden, supporting the applicability of this combinatorial strategy in tumors with low mutational burden such as OC.<sup>38</sup>

Overall, the results provided by this study demonstrate CD8CD103 double staining as a superior tool for prognostication compared to single CD8 or CD103 and advocates the further exploration of image-based quantification of CD8CD103 TRM in HGSO. We demonstrate that the prognostic benefit of CD8CD103 TRM infiltration in HGSO is restricted to PDS treated patients with a complete debulking. This approach provides novel insights into prognostic stratification of HGSO patients and may contribute to personalized treatment strategies in the future.

## Declaration of Interest statements

**MJ**, Advisory Board, honoraria to institution: Merck, BMS, Novartis, Pierre Fabre, Tesaro, AstraZeneca. Clinical studies: BMS, AbbieVie, Merck, Cristal Therapeutics

**VHK**, V.H. Koelzer reports grants from Promedica Foundation (F-87701-41-01) during the conduct of the study, and has served as an invited speaker on behalf of Indica Labs.

**MB**, Outside the submitted work, dr. de Bruyn reports grants from the Dutch Cancer Society (KWF), grants from the European Research Council (ERC), grants from Health Holland, grants from DCPrime, non-financial support from BioNTech, non-financial support from SurfRay, grants and non-financial support from Vicinivax; In addition, dr. de Bruyn has grants and non-financial support from Aduro Biotech, in part relating to a patent for Antibodies targeting CD103 (de Bruyn et al. No. 62/704,258).

**HWN**, Outside the submitted work, prof. Nijman reports grants from the Dutch Cancer Society (KWF), grants from Health Holland, non-financial support from AIMM Therapeutics, grants from DCPrime, non-financial support from BioNTech, grants and shares and non-financial support from Vicinivax; In addition, prof. Nijman has grants and non-financial support from Aduro Biotech, in part relating to a patent for Antibodies targeting CD103 (de Bruyn et al. No. 62/704,258).

## Disclosure of potential conflicts of interest

There are no conflicts of interest to disclose for the remaining author(s).

## Funding

The study is supported by the Dutch Cancer Society: project grant RUG 2015-7235.

## ORCID

G. B. A. Wisman  <http://orcid.org/0000-0002-4830-3401>

H. W. Nijman  <http://orcid.org/0000-0002-1821-3042>

## References

1. Lheureux S, Gourley C, Vergote I, Oza AM. Epithelial ovarian cancer [Internet]. The Lancet. Lancet Publishing Group. 2019 [accessed 2020 Nov 10];393:1240–1253. <https://pubmed.ncbi.nlm.nih.gov/30910306/>.
2. Webb PM, Jordan SJ. Epidemiology of epithelial ovarian cancer. Best Pract Res. Bailliere Tindall Ltd. 2017;41:3–14. doi:10.1016/j.bpobgyn.2016.08.006.
3. Vaughan S, Coward JI, Bast RCJ, Berchuck A, Berek JS, Brenton JD, Coukos G, Crum CC, Drapkin R,

- Etemadmoghadam D, et al. Rethinking ovarian cancer: recommendations for improving outcomes. *Nat Rev Cancer*. 2011 Sept;11(10):719–725. doi:10.1038/nrc3144.
4. Colombo N, Sessa C, Du Bois A, Ledermann J, McCluggage WG, McNeish I, Morice P, Pignata S, Ray-Coquard I, Vergote I, et al. ESMO-ESGO consensus conference recommendations on ovarian cancer: pathology and molecular biology, early and advanced stages, borderline tumours and recurrent disease. *Ann Oncol* [Internet]. 2019 [accessed 2020 Oct 27];30(5):672–705. <https://pubmed.ncbi.nlm.nih.gov/31046081/>.
  5. Eggink FA, Koopmans CM, Nijman HW. Surgery for patients with newly diagnosed advanced ovarian cancer: which patient, when and extent? *Curr Opin Oncol*. Lippincott Williams and Wilkins. 2017;29:351–358. doi:10.1097/CCO.0000000000000387.
  6. Gooden MJM, De Bock GH, Leffers N, Daemen T, Nijman HW. The prognostic influence of tumour-infiltrating lymphocytes in cancer: a systematic review with meta-analysis. *Br J Cancer*. 2011;105:93–103. doi:10.1038/bjc.2011.189.
  7. Leffers N, Gooden MJM, de Jong RA, B-n H, ten Hoor KA, Hollema H, Boezen HM, Van Der Zee AGJ, Daemen T, Nijman HW, et al. Prognostic significance of tumor-infiltrating T-lymphocytes in primary and metastatic lesions of advanced stage ovarian cancer. *Cancer Immunol Immunother*. 2009 Mar;58(3):449–459. doi:10.1007/s00262-008-0583-5.
  8. Zhang L MD, Conejo-Garcia JR M.D. PD, Katsaros D M.D. PD, Gimotty PA PD, Massobrio M MD, Regnani G MD, Makrigiannakis A, Gray H, Schlienger K, Liebman MN, et al. Intratumoral T cells, recurrence, and survival in epithelial ovarian cancer. *New Engl J Med*. 2003;348(48):203–213. doi:10.1056/NEJMoa020177.
  9. Kim Y, Shin Y, Kang GH. Prognostic significance of CD103+ immune cells in solid tumor: a systemic review and meta-analysis. *Sci Rep*. 2019 Dec;9(1):1–7. doi:10.1038/s41598-018-37186-2.
  10. Webb JR, Milne K, Nelson BH. PD-1 and CD103 are widely coexpressed on prognostically favorable intraepithelial CD8 T cells in human ovarian cancer. *Cancer Immunol Res*. 2015 Aug;3(8):926–935. doi:10.1158/2326-6066.CIR-14-0239.
  11. Komdeur FL, Prins TM, Van De Wall S, Plat A, Wisman GBA, Hollema H, Daemen T, Church DN, de Bruyn M, Nijman HW, et al. CD103+ tumor-infiltrating lymphocytes are tumor-reactive intraepithelial CD8+ T cells associated with prognostic benefit and therapy response in cervical cancer. *Oncoimmunology*. 2017;6(9):e1338230. doi:10.1080/2162402X.2017.1338230.
  12. Workel HH, Komdeur FL, Wouters MCA, Plat A, Klip HG, Eggink FA, Wisman GBA, Arts HJG, Oonk MHM, Mourits MJE, et al. CD103 defines intraepithelial CD8+ PD1+ tumour-infiltrating lymphocytes of prognostic significance in endometrial adenocarcinoma. *Eur J Cancer*. 2016 June;60:1–11. doi:10.1016/j.ejca.2016.02.026.
  13. Ganesan AP, Clarke J, Wood O, Garrido-Martin EM, Chee SJ, Mellows T, Samaniego-Castruita D, Singh D, Seumois G, Alzetani A, et al. Tissue-resident memory features are linked to the magnitude of cytotoxic T cell responses in human lung cancer. *Nat Immunol* [Internet]. 2017 July 19 [accessed 2021 May 5];18(8):940–950. <https://pubmed.ncbi.nlm.nih.gov/28628092/>.
  14. Franciszkiewicz K, Le Floch A, Boutet M, Vergnon I, Schmitt A, Mami-Chouaib F. CD103 or LFA-1 engagement at the immune synapse between cytotoxic T cells and tumor cells promotes maturation and regulates T-cell effector functions. *Cancer Res* [Internet]. 2013 Jan 15 [accessed 2021 May 5];73(2):617–628. <http://cancerres.aacrjournals.org/>.
  15. Workel HH, Lubbers JM, Arnold R, Prins TM, van der Vlies P, de Lange K, Bosse T, Van Gool IC, Eggink FA, Wouters MCA, et al. A transcriptionally distinct CXCL13+CD103+CD8+T-cell population is associated with b-cell recruitment and neoantigen load in human cancer. *Cancer Immunol Res* [Internet]. 2019 May 1 [accessed 2021 May 5];7(5):784–796. <https://pubmed.ncbi.nlm.nih.gov/30872264/>.
  16. Hamilton PW, van Diest PJ, Williams R, Gallagher AG. Do we see what we think we see? The complexities of morphological assessment. *J Pathol*. 2009 July;218(3):285–291. doi:10.1002/path.2527.
  17. Levine AB, Schlosser C, Grewal J, Coope R, Jones JM, Stephen Yip S. Rise of the machines: advances in deep learning for cancer diagnosis. *Cell* [Internet]. 2019;5(3):157–169. <https://www.scienceirect.com/science/article/pii/S2405803319300184?via%3Dihub>.
  18. Bychkov D, Linder N, Turkki R, Nordling S, Kovanen PE, Verrill C, Walliander M, Lundin M, Haglund C, Lundin J, et al. Deep learning based tissue analysis predicts outcome in colorectal cancer. *Sci Rep*. 2018 Dec;8(1):1–11. doi:10.1038/s41598-018-21758-3.
  19. Koelzer VH, Sirinukunwattana K, Rittscher J, Mertz KD. Precision immunoprofiling by image analysis and artificial intelligence [Internet]. *Virchows Arch*. Springer Verlag. 2019 [accessed 2020 Oct 27];474:511–522. <https://pubmed.ncbi.nlm.nih.gov/30470933/>.
  20. Horeweg N, de Bruyn M, Nout RA, Stelloo E, Kedzierska KZ, León-Castillo A, Plat A, Mertz KD, Osse M, Jürgenliemk-Schulz IM, et al. Prognostic integrated image-based immune and molecular profiling in early-stage endometrial cancer. *Cancer Immunol Res*. 2020 Sept;canimm.0149.2020. doi:10.1158/2326-6066.CIR-20-0149.
  21. Wouters MCA, Komdeur FL, Workel HH, Klip HG, Plat A, Kooi NM, Wisman GBA, Mourits MJE, Arts HJG, Oonk MHM, et al. Treatment regimen, surgical outcome, and T-cell differentiation influence prognostic benefit of tumor-infiltrating lymphocytes in high-grade serous ovarian cancer. *Clin Cancer Res*. 2016 Feb;22(3):714–724. doi:10.1158/1078-0432.CCR-15-1617.
  22. Tseng JH, Cowan RA, Zhou Q, Iasonos A, Byrne M, Polcino T, Polen-De C, Gardner GJ, Sonoda Y, Zivanovic O, et al. Continuous improvement in primary Debulking surgery for advanced ovarian cancer: do increased complete gross resection rates independently lead to increased progression-free and overall survival? *Gynecol Oncol*. 2018 Oct;151(1):24–31. doi:10.1016/j.ygyno.2018.08.014.
  23. Cobb LP, Sun CC, Iyer R, Nick AM, Fleming ND, Westin SN, Sood AK, Wong KK, Silva EG, Gershenson DM, et al. The role of neoadjuvant chemotherapy in the management of low-grade serous carcinoma of the ovary and peritoneum: further evidence of relative chemoresistance. *Gynecol Oncol* [Internet]. 2020;158:653–658. doi:10.1016/j.ygyno.2020.06.498.
  24. Martin SD, Brown SD, Wick DA, Nielsen JS, Kroeger DR, Twumasi-Boateng K, Holt RA, Nelson BH. Low mutation burden in ovarian cancer may limit the utility of neoantigen-targeted vaccines. *PLoS One*. 2016;11(5):1–22. doi:10.1371/journal.pone.0155189.
  25. Alexandrov LB, Nik-Zainal S, Wedge DC, Aparicio SAJR, Behjati S, Biankin AV, Bignell GR, Bolli N, Borg A, Børresen-Dale A-L, et al. Signatures of mutational processes in human cancer. *Nature*. 2013;500(7463):415–421. doi:10.1038/nature12477.
  26. Zhang L, Conejo-Garcia JR, Katsaros D, Gimotty PA, Massobrio M, Regnani G, Makrigiannakis A, Gray H, Schlienger K, Liebman MN, et al. Intratumoral T cells, recurrence, and survival in epithelial ovarian cancer. *N Engl J Med*. 2003 Jan;348(3):203–213.
  27. Brunekreef KL, Paijens ST, Wouters MCA, Komdeur FL, Eggink FA, Lubbers JM, Workel HH, Van Der Slikke EC, Pröpper NEJ, Leffers N, et al. Deep immune profiling of ovarian tumors identifies minimal MHC-I expression after neoadjuvant chemotherapy as negatively associated with T-cell-dependent outcome. *Oncoimmunology*. 2020 Jan;9(1):1760705. doi:10.1080/2162402X.2020.1760705.
  28. Garcia-Lora A, Algarra I, Garrido F. MHC class I antigens, immune surveillance, and tumor immune escape. *J Cell Physiol*. 2003 June;195(3):346–355. doi:10.1002/jcp.10290.
  29. Rosato PC, Wijeyesinghe S, Stolley JM, Nelson CE, Davis RL, Manlove LS, Pennell CA, Blazar BR, Chen CC, Geller MA, et al. Virus-specific memory T cells populate tumors and can be repurposed for tumor immunotherapy. *Nat Commun* [Internet]. 2019 Dec 1 [accessed 2020 Oct 27];10(1). <https://pubmed.ncbi.nlm.nih.gov/30718505/>.
  30. Borella F, Ghisoni E, Giannone G, Cosma S, Benedetto C, Valabrega G, Katsaros D. Immune checkpoint inhibitors in

- epithelial ovarian cancer: an overview on efficacy and future perspectives [Internet]. *Diagnostics* MDPI AG; 2020 [accessed 2020 Oct 6]. p. 146. 10(3):. [/pmc/articles/PMC7151145/?report=abstract](https://pmc/articles/PMC7151145/?report=abstract).
31. Matulonis UA, Shapira-Frommer R, Santin AD, Lisyanskaya AS, Pignata S, Vergote I, Raspagliesi F, Sonke GS, Birrer M, Provencher DM, et al. Antitumor activity and safety of pembrolizumab in patients with advanced recurrent ovarian cancer: results from the phase II KEYNOTE-100 study. *Ann Oncol* [Internet]. 2019 July 1 [accessed 2020 Oct 6];30(7):1080–1087. <https://pubmed.ncbi.nlm.nih.gov/31046082/>.
  32. Hamanishi J, Mandai M, Ikeda T, Minami M, Kawaguchi A, Murayama T, Kanai M, Mori Y, Matsumoto S, Chikuma S, et al. Safety and antitumor activity of Anti-PD-1 antibody, nivolumab, in patients with platinum-resistant ovarian cancer. *J Clin Oncol* [Internet]. 2015 Dec 1 [accessed 2020 Oct 7];33(34):4015–4022. <https://pubmed.ncbi.nlm.nih.gov/26351349/>.
  33. Blank CU, Rozeman EA, Fanchi LF, Sikorska K, van de Wiel B, Kvistborg P, Krijgsman O, van den Braber M, Philips D, Broeks A, et al. Neoadjuvant versus adjuvant ipilimumab plus nivolumab in macroscopic stage III melanoma. *Nat Med*. 2018 Nov;24(11):1655–1661. doi:10.1038/s41591-018-0198-0.
  34. Versluis JM, Long GV, Blank CU. Learning from clinical trials of neoadjuvant checkpoint blockade. *Nat Med*. 2020 Apr;26(4):475–484. doi:10.1038/s41591-020-0829-0.
  35. Schachter J, Ribas A, Long GV, Arance A, Grob JJ, Mortier L, Daud A, Carlino MS, McNeil C, Lotem M, et al. Pembrolizumab versus ipilimumab for advanced melanoma: final overall survival results of a multicentre, randomised, open-label phase 3 study (KEYNOTE-006). *Lancet*. 2017 Oct;390(10105):1853–1862. doi:10.1016/S0140-6736(17)31601-X.
  36. Borghaei H, Paz-Ares L, Horn L, Spigel DR, Steins M, Ready NE, Chow LQ, Vokes EE, Felip E, Holgado E, et al. Nivolumab versus docetaxel in advanced nonsquamous non-small-cell lung cancer. *N Engl J Med*. 2015 Oct;373(17):1627–1639. doi:10.1056/NEJMoa1507643.
  37. Chalabi M, Fanchi LF, Dijkstra KK, Van Den Berg JG, Aalbers AG, Sikorska K, Lopez-Yurda M, Grootsholten C, Beets GL, Snaebjornsson P, et al. Neoadjuvant immunotherapy leads to pathological responses in MMR-proficient and MMR-deficient early-stage colon cancers. *Nat Med*. 2020 Apr;26(4):566–576. doi:10.1038/s41591-020-0805-8.
  38. Sahin U, Oehm P, Derhovanessian E, Jabulowsky RA, Vormehr M, Gold M, Maurus D, Schwarck-Kokarakis D, Kuhn AN, Omokoko T, et al. An RNA vaccine drives immunity in checkpoint-inhibitor-treated melanoma. *Nature*. 2020;585(7823):107–112. doi:10.1038/s41586-020-2537-9.